Published in final edited form as:
Nature. 2018 March 21; 555(7697): 507–510. doi:10.1038/nature25990.

Isotopic evolution of the protoplanetary disk and the building blocks of Earth and Moon

Martin Schiller[1], **Martin Bizzarro**[1], and **Vera Assis Fernandes**[2,3]

[1]Centre for Star and Planet Formation and Natural History Museum of Denmark, University of Copenhagen, Øster Voldgade 5–7, DK-1350, Denmark

[2]Museum für Naturkunde, Leibniz-Institut für Evolutions- und Biodiversitätsforschung, Berlin 10115, Germany

[3]Instituto Dom Luiz, Faculdade de Ciências, Universidade de Lisboa, 1749-016 Lisboa, Portugal

Abstract

Nucleosynthetic isotope variability amongst Solar System objects is commonly used to probe the genetic relationship between meteorite groups and rocky planets, which, in turn, may provide insights into the building blocks of the Earth-Moon system1–5. Using this approach, it is inferred that no primitive meteorite matches the terrestrial composition such that the nature of the disk material that accreted to form the Earth and Moon is unconstrained6. This conclusion, however, is based on the assumption that the observed nucleosynthetic variability amongst inner Solar System objects predominantly reflects spatial heterogeneity. Here, we use the isotopic composition of the refractory element calcium to show that the inner Solar System's nucleosynthetic variability in the mass-independent $^{48}Ca/^{44}Ca$ ratio ($\mu^{48}Ca$) primarily represents a rapid change in the $\mu^{48}Ca$ composition of disk solids associated with early mass accretion to the proto-Sun. In detail, the $\mu^{48}Ca$ values of samples originating from the ureilite and angrite parent bodies as well as Vesta, Mars and Earth are positively correlated to the masses of the inferred parent asteroids and planets – a proxy of their accretion timescales – implying a secular evolution of the bulk $\mu^{48}Ca$ disk composition in the terrestrial planet-forming region. Individual chondrules from ordinary chondrites formed within 1 Myr of proto-Sun collapse7 record the full range of inner Solar System $\mu^{48}Ca$ compositions, indicating a rapid change in the composition of the disk material. We infer that this secular evolution reflects admixing of pristine outer Solar System material to the thermally-processed inner protoplanetary disk associated with the accretion of mass to the proto-Sun. The indistinguishable $\mu^{48}Ca$ composition of the Earth (0.2±3.9 ppm) and Moon (3.7±1.9

Correspondence and requests for materials should be addressed to M.S. (schiller@snm.ku.dk).

Author Contributions M.S. and M.B. designed the study and experiments. M.S. conducted the analytical work. All authors participated in the interpretation of the data. M.S. and M.B wrote the manuscript with input from V.A.F.

Author Information Reprints and permissions information is available at www.nature.com/reprints. Readers are welcome to comment on the online version of the paper.

The author declares no competing financial interests.

Data availability The authors declare that data supporting the findings of this study are available within the paper, the methods, its Extended Data and from the EarthChem library (http://dx.doi.org/10.1594/IEDA/100744).

Europe PMC Funders Author Manuscripts

ppm) reported here is a prediction of our model if the Moon-forming impact involved protoplanets or precursors that completed their accretion near the end of the disk lifetime.

Protoplanetary disks form as a result of mass accretion from the collapsing envelope onto the star. The rate of mass accretion onto the star via the disk is typically high in the early stages, resulting in elevated temperatures within a few astronomical units (AU) of the star8. In the Solar System, mass accretion to the proto-Sun resulted in thermal processing of pristine infalling molecular cloud material, including the selective destruction of presolar carriers of nucleosynthetic isotope anomalies. This process is expressed by correlated variability in the abundance of nuclides of distinct nucleosynthetic origin such as ^{46}Ti-^{50}Ti and ^{43}Ca-^{46}Ca-^{48}Ca amongst Solar System reservoirs2,3. Parent bodies of meteorites formed from inner, thermally-processed, disk material record depletions in these isotopes relative to bodies formed in the outer disk regions. The mass-independent isotopic compositions of various elements can thus fingerprint the source of the precursor material to terrestrial planets. However, this requires understanding the secular evolution of the nucleosynthetic composition of the disk material that accreted to growing planetary bodies. Unlike nucleosynthetic tracers present as trace elements in planets (Ti and Cr) or siderophile elements (Mo and Ru) that track the source of the metal fraction of a body, calcium is a major constituent of rock-forming minerals and, hence, provides robust constraints on the precursor material to rocky planets. To probe the Ca isotope evolution of the protoplanetary disk, we determined the mass-independent ^{48}Ca isotope composition of strategically-selected Solar System objects, including ordinary and carbonaceous chondrites, ureilites, eucrites, angrites, martian and lunar meteorites as well as individual chondrules from ordinary and carbonaceous chondrites (Fig. 1).

The growth of asteroids and Mars-sized embryos can result from the gas-drag-assisted accretion of mm-sized chondrules within ~3 Myr9,10. The U-corrected Pb-Pb ages and initial Pb isotopes of the chondrules we investigated indicate a primary formation age restricted to the first Myr of disk evolution, although some objects have been remelted at later times7. These chondrules provide insights into the spatial and temporal evolution of the μ^{48}Ca composition of disk solids at early times (Fig. 1). The CR chondrules record μ^{48}Ca compositions comparable to CI chondrites, indicating that their precursor material escaped extensive thermal processing. In contrast, ordinary chondrite chondrules record variable μ^{48}Ca compositions ranging from the terrestrial value to deficits of –161±27 ppm. Our bulk meteorite data are consistent with earlier studies3,11, namely that bodies formed in the inner disk show systematic depletions in μ^{48}Ca whereas carbonaceous outer Solar System bodies record excesses relative to Earth (Fig. 1).

Given the analytical uncertainty of the individual chondrule ages, it is difficult to distinguish between a model where the deficits in μ^{48}Ca relative to the solar composition reflect spatial heterogeneity or temporal evolution of the bulk composition of inner disk solids. Astronomical observations of young stars and their disks indicate that the main accretion epoch of thermally-unprocessed envelope material occurs over timescales comparable to those of primary chondrule formation, namely during the first Myr of disk evolution12. Accepting that CI chondrites approximate the average composition of the envelope material,

Europe PMC Funders Author Manuscripts

admixing this material to the inner disk will result in a progressive increase in the $\mu^{48}Ca$ composition of solids and bodies formed during this epoch. To test this hypothesis, we turn to the ^{48}Ca composition of differentiated asteroids and planetary bodies, as their $\mu^{48}Ca$ values reflect the average compositions of their precursors throughout the bodies´ accretion history.

Recent models9,10 for the formation and growth of asteroidal bodies and planetary embryos suggest a two stage process, where first generation bodies with characteristic sizes of ~100 km form rapidly by streaming instabilities followed by continuous growth that is dominated by the gas-drag assisted accretion of mm-sized particles for bodies with radii larger than ~200 km. This results in the formation of Mars-sized embryos over typical disk lifetimes of less than 5 Myr. Importantly, formation of the first embryos leads to the excitation of the inclinations of the smaller asteroids, which disconnects the asteroids from the chondrules in the mid-plane layer and, hence, terminates their accretion. Assuming a similar rate of accretion in the terrestrial planet forming region, a consequence of these models is that the final mass of a rocky body is a function of its accretion timescale. Whereas the masses of Earth, Mars and Vesta (the howardite-eucrite-diogenite parent body13) can be inferred, the parent bodies of ureilites and angrites meteorites are not known. However, the presence of a core dynamo in the angrite parent body14, a magmatic differentiation and volcanic evolution indicating a similar thermal history to Vesta15,16 and the retention of basaltic lavas on its surface suggests the angrite parent body may have been comparable in size to Vesta. The mass of the ureilite parent body was calculated using a density of 3.22 g cm^{-3} and a radius of 105±25 km17,18. We note that the absence of basaltic meteorites from the ureilite parent body, possibly indicating loss of basaltic lavas via explosive volcanism, is consistent with a radius ≤100 km for this body19. Figure 2A shows that the ^{48}Ca composition of inner Solar System differentiated bodies systematically increases with their masses, indicating a secular evolution of the time-integrated average ^{48}Ca composition of the disk material that accreted to form the terrestrial planets. Thus, the inner disk ^{48}Ca nucleosynthetic variations are best understood as predominantly reflecting progressive admixing of pristine, outer Solar System matter to an initially thermally-processed dust reservoir during the early stage of disk evolution. This establishes that the nucleosynthetic variability recorded by inner disk bodies is primarily controlled by the formation timescales of their precursors. This interpretation is also generally consistent with other nucleosynthetic tracers of lithophile affinity when considering the uncertainties of the data (see methods).

The inner Solar System chondrules investigated here suggest that the $\mu^{48}Ca$ of disk solids evolved from an ureilite-like to a terrestrial composition within ~1 Myr of Solar System formation. Whereas these data indicate a rapid isotopic evolution of accreting disk solids, they provide no constraints on the rate of change of the average bulk composition of the inner disk. However, this information can be inferred from the $\mu^{48}Ca$ of differentiated asteroids and planetary bodies as their composition reflects the time-integrated average of the disk composition at the time of their accretion. Two ordinary chondrite chondrules with U-corrected Pb-Pb ages within ~100,000 years of Solar System formation record $\mu^{48}Ca$ compositions identical to the most depleted $\mu^{48}Ca$ value defined by a differentiated asteroid, namely the ureilite parent body. Short-lived radionuclide chronology and thermal modeling indicate that the ureilite parent body completed its accretion <100,000 years of Solar System

formation (see methods). Collectively, these observations suggest that the ureilite μ^{48}Ca value of –146±14 ppm represents that of the inner disk dust reservoir initially depleted in ^{48}Ca through thermal processing. When Vesta and the angrite parent bodies accreted <0.25±0.15 Myr of Solar System formation20,21, the time-integrated average μ^{48}Ca of inner disk rocky bodies had evolved to –93.2±7.1 ppm and, lastly, to –20.0±2.8 and 0.2±3.9 ppm when Mars and Earth's precursors completed their accretion, respectively.

It is well-established that the protoplanetary disk was dissipated at the time of formation of the impact-generated Gujba CB chondrules at 4562.49±0.21 Ma22, implying cessation of infall of outer Solar System material to the inner disk. Thus, the timing of disk dissipation marks the transition when the μ^{48}Ca composition of inner disk bodies can no longer be modified by infall. Given the observed relationship between μ^{48}Ca values and planetary masses (Fig. 2A), the timing of accretion of Earth's precursor can be deduced assuming that the accretion timescales of Mars, Vesta as well as angrite and ureilite parent bodies are well understood. The Hf-W systematics of martian meteorites suggest that Mars reached half of its mass by $1.8^{+0.9}_{-1.0}$ Myr23, whereas thermal modelling and ^{26}Al-^{26}Mg data constrain the accretion of Vesta and the angrite parent body <0.4 Myr of CAI formation20,21. Accretion of the ureilite parent body is believed to have been completed by ~0.1 Myr to ensure partial differentiation from the decay of ^{26}Al (see methods). Using these estimates, we show in Fig. 2B that accretion of the proto-Earth or its precursors, which may include a number of planetary embryos (see Fig. 2 caption), was completed by ~5.3 Myr. Collectively, these observations suggest that the μ^{48}Ca value of Earth represents the average bulk inner disk composition prior to its dissipation. The addition rate of outer Solar System material to the inner disk can be evaluated from the secular change in the average μ^{48}Ca inner disk composition inferred from differentiated asteroids and planets. Accepting an ureilite-like μ^{48}Ca value for the bulk inner disk at 0.1 Myr, we show in Fig. 3A that the rate of addition of outer Solar System material to the inner disk mirrors the typical mass accretion rates of low mass protostars24. Thus, the flux of outer Solar System material to the inner disk appears associated with infall of envelope material and, hence, growth of the proto-Sun.

Our model for the secular μ^{48}Ca evolution of the inner protoplanetary disk provides insights into the nature of the precursor material to planetesimals and planets. The compositions of Vesta and the angrite parent body requires admixing of 15% of thermally-unprocessed CI-like material to their precursors. For Mars and the proto-Earth, the amount of thermally-unprocessed material needed to account for their bulk μ^{48}Ca compositions is 36% and 42%, respectively. If correct, this implies that more than half of the mass of the inner disk was already locked into asteroidal bodies and/or planetary embryos ~100,000 years after proto-Sun collapse (Fig. 3B). Thus, the μ^{48}Ca composition of terrestrial planets preserves a record of their accretion history throughout the entire disk lifetime. In contrast, most chondrites represent fragments of late accreted bodies and, as such, can at best only represent a snapshot of a disk composition at the time of their accretion. However, given the small size of their parent bodies, it is unclear if their compositions are representative of that of the average accreting material at the time of their formation, which can be also influenced by variable proportions of chondrule and matrix. For example, the ordinary chondrite chondrules analysed here record a weighted average μ^{48}Ca of –129±50 ppm, making the

bulk rock composition very sensitive to the chondrule to matrix ratio. Thus, chondrites cannot be used to faithfully assess the nature of the precursor material to rocky planets.

To explain the observed nucleosynthetic dichotomy between inner and outer Solar System bodies, Kruijer *et al.*25 proposed that transport of outer Solar System material to the inner disk was stopped by the opening of a disk gap related to the formation Jupiter's core ~1 Myr after formation of the Sun. However, numerical simulations and astronomical observations suggest that opening of a disk gap does not quench mass accretion to the protostar but rather limits the inward transport of large dust grains by filtration26,27. Coagulation of smaller dust particles sunward of the disk gap will continue to fuel planetary growth by pebble accretion. The apparent lack of this material in ordinary chondrites may reflect the fact that the main growth mechanism of small bodies, namely the streaming instability, is less efficient in accreting smaller particles. Testing this hypothesis, however, requires numerical simulation to better understand size sorting during planetesimal formation by the streaming instability relative to size sorting by pebble accretion. Lastly, our results and interpretations imply that more than half of the mass of the inner disk was already locked into sizeable bodies with a $\mu^{48}Ca$ composition akin to ureilites ~100,000 years after proto-Sun collapse (Fig. 3B). Mass balance arguments indicate that admixing of pristine outer Solar System CI-like dust to this inner disk reservoir can at most raise the bulk $\mu^{48}Ca$ disk value to approximately the terrestrial composition, thereby preserving a contrast between rocky planets and carbonaceous asteroidal bodies. Thus, we infer that the nucleosynthetic dichotomy between inner and outer Solar System bodies reflects the rapid accretion of thermally-processed disk material into asteroidal bodies and/or planetary embryos and does not require the early formation of a disk gap.

The giant impact theory for the formation of the Earth-Moon system proposes that a Mars-sized embryo collided with the proto-Earth and ejected material into an Earth-orbiting disk, which subsequently accumulated into the Moon28. Since models predict that most of the Moon's mass is derived from the impactor, this theory is difficult to reconcile with the near identical isotopic composition of the Earth and Moon for lithophile elements1,5,29. As such, a number of alternate models have been proposed that allow for disk-planet compositional equilibration to occur30–32. Our high-precision data define a $\mu^{48}Ca$ value for the Moon of 3.7±1.9 ppm relative to Earth, requiring the ^{48}Ca compositions of the proto-Earth and the impactor in the framework of the canonical model29 to be within 10 ppm. As our results suggest that the bulk ^{48}Ca composition of the inner protoplanetary disk evolved to a terrestrial composition within ~5 Myr (Fig. 2B), the isotopic similarity between the Earth and Moon can be easily understood if the giant impact involved bodies or precursors that completed their accretion towards the end of the disk lifetime. The nearly identical isotope signature of the Earth and the Moon is not fortuitous but rather an outcome of the evolving isotopic composition of the disk.

Methods

Sample preparation and isotope analyses

Bulk samples, weighing between 20 and 100 mg, were digested in a HF-HNO_3 media in Parr bombs at 210°C for 2-3 days. Calcium was also separated from sample digestions of

nine chondrules extracted from the ordinary chondrite (L3.10) NWA 5697 and two chondrules from the CR2 NWA 6043 that have previously been analysed for Pb isotopes7. The individual sample dissolutions typically represent <10 mg of sampled chondrule material, which is significantly smaller than the amount of processed bulk meteorite samples. Following complete dissolution of the samples, Ca was purified in a four-step procedure from the sample matrix by ion exchange chromatography34. Although this procedure normally results in an efficient separation of Ca from the sample matrix, all samples were monitored for the presence of contaminant elements in the purified Ca solution such as Mg, Sr and Ti. Individual chromatography separation steps were repeated for samples where the presence of contaminants was considered to have a potential impact on the analysis (e.g. Sr/Ca > 1×10^{-6}). Isotopic compositions of the purified Ca separates were measured with the Neptune Plus multiple collector – inductively coupled plasma – mass spectrometer (MC-ICPMS) at the Centre for Star and Planet Formation (Natural History Museum of Denmark, University of Copenhagen) following established analytical procedures3,34. Calcium isotope data were acquired in static mode using six Faraday collectors set-up as follows: ^{48}Ca, ^{47}Ti, and ^{46}Ca in the high-4, high-2 and high-1 collectors, respectively, on the high mass side of the axial Faraday and ^{42}Ca, ^{43}Ca and ^{44}Ca in the low-4, low-2, and low-1 collector, respectively on the low mass side of the axial Faraday. The high-2 collector Faraday cup (^{47}Ti) was connected to an amplifier with a 10^{12} Ω feedback resistor, whereas the remaining collectors were connected to amplifiers with 10^{11} Ω feedback resistors. Samples were aspirated into the plasma source by means of an Apex sample introduction system with an uptake rate of 20 μL/min and Ca isotopes were measured with a mass resolving power (M/ΔM as defined by the peak edge width from 5% to 95% full peak height) that was always greater than 5000. The sensitivity under these analytical conditions was approximately 300 V ppm^{-1}.

Given the low abundance of the ^{46}Ca nuclide as well as the limited μ^{43}Ca variability between bulk inner Solar System reservoirs (<20 ppm) relative to the measurement uncertainty (~2 ppm)3,34, we focus in this work on the high-precision determination of the mass-independent component of ^{48}Ca (μ^{48}Ca), which we measure with an external reproducibility of 12 ppm for individual sample analyses34. We also report the mass-dependent ^{42}Ca/^{44}Ca ($\delta^{42/44}$Ca) and ^{43}Ca/^{44}Ca ($\delta^{43/44}$Ca) values with respect to SRM 915b in the delta notation that are obtained alongside the μ^{48}Ca data. Single analyses for each sample of sufficient size consist of 15-20 sample measurements comprising a total of 839 s of data acquisition and 340 s of baseline bracketed by measurements of the SRM 915b standard. For individual chondrules both signal intensity and number of repeat analyses were adjusted to achieve the best possible precision given the limited amount of Ca available for these samples. All data reduction was conducted off-line and changes in mass bias with time were interpolated using a smoothed cubic spline. For each analysis the mean and standard error of the measured ratios were calculated using a 3SD threshold to reject outliers. Individual analyses of a sample were combined to produce an average weighted by the propagated uncertainties of individual analyses and reported final uncertainties are 2 times the standard error (2SE) of the mean.

Calculation of disk mass accretion rates

For simplicity, we assume that the mass of the asteroids, moons and planets sunward of Jupiter represents the final mass of the protoplanetary disk and the ^{48}Ca signature of Earth, which makes up 50% of this mass, is representative of the final inner disk composition. This assumption is justified as the μ^{48}Ca values track the composition of disk solids and not that of the gas. The mass accreted in bodies at any given time is assumed to be traced by the bulk μ^{48}Ca signature of planetary bodies, where increase in the ^{48}Ca of planetary bodies represents an addition of outer Solar System material to the growing inner disk. In this simple two-component mixing model, the ureilite parent body represents the mean composition of the inner disk at 0.1 Myr after the formation of the Solar System. The ^{48}Ca signature of CI chondrites represents the added outer Solar System material during the lifetime of the disk and the ^{48}Ca signature of the Earth the final composition of the disk after accretion has ceased. This mixing model requires 58.4% of the material has accreted by the time the ureilite parent body formed (<0.1 Myr). The subsequent increase in bulk ^{48}Ca signatures of Vesta and the angrite parent body, Mars at half of its current mass and proto-Earth represent addition of 15.0%, 19.6% and 6.9% outer Solar System material during the time intervals between accretion of the 1) the ureilite parent body and Vesta (between 0.1 Myr to 0.4 Myr), 2) Vesta and Mars at 50% of its mass (between 0.4 to 2.7 Myr) and 3) Mars at 50% of its mass and proto-Earth (between 2.7 to 5.3 Myr), respectively. The amount of early-accreted material only increases if the ^{48}Ca signature of other carbonaceous chondrites is assumed rather than that of CI chondrites. The change in accreted mass per time interval relative to the final disk mass (i.e. 0.584, 0.150, 0.196 and 0.069 of the final inner disk mass) allows us to calculate mean inner disk mass accretion rates for each of the four interval's by dividing the added mass per time interval by its duration (0.1, 0.3, 2.3 and 2.6 Myr). Resulting accretion rates are 5.8×10^{-6}, 5.0×10^{-7}, 8.5×10^{-8} and 2.6×10^{-8} $M_{inner\ disk}$/yr, respectively.

Timing of accretion of the ureilite parent body

The energy release from the decay of the short-lived ^{26}Al radionuclide ($t_{1/2}$ = 0.73 Myr) is the most important heat source driving differentiation on small planetary bodies accreted during the first few Myr of our Solar System's formation. Thus, determining the timing of accretion of differentiated bodies can be inferred by estimating the time needed for the parent body to achieve global melting from the energy released by ^{26}Al, which requires knowledge of the timing of differentiation as well as the initial abundance of ^{26}Al the body's precursor material. Recent studies have shown that canonical levels of ^{26}Al found in calcium-aluminum-rich inclusions (CAIs) are not representative for the majority of the matter that made up the terrestrial planet forming region21,35. Instead, ^{26}Al/^{27}Al values in this region at the time of CAI formation were more likely characterized by values between 1 and 1.6×10^{-5} (ref. 21,35). Based on ^{26}Al-^{26}Mg and ^{53}Mn-^{53}Cr systematics the timing of initial magmatic differentiation on the ureilite parent body took place at 4567.1±1.1. Myr ago36,37, indistinguishable from the age of our Solar System based on CAIs38. Accepting that the initial abundance of ^{26}Al/^{27}Al in the material from which the ureilite parent body formed was 1.3×10^{-5} and the precursor material was ordinary chondrite-like in density and composition, thermal modeling requires that the accretion must have been completed by 0.1 Myr after CAI formation. This is constrained by assuming an ambient temperature of 550 K

in the accretion region of the ureilite parent body at ~0.1 Myr39 and requires the parent body to achieve an internal temperature of 1553K equivalent to 30% partial melting18 within 1.1 Myr after CAI formation, which is the time allowed by the age uncertainty for magmatic differentiation36,37. We note that this accretion age is consistent with independent estimates of the accretion time of the ureilite parent body40.

Stable Ca isotope composition of meteorites and chondrules

We report $\delta^{42/44}$Ca and $\delta^{43/44}$Ca values for each individual sample as the per mil deviations from SRM 915b in the Extended Data Table 1 and Extended Data Figure 2 given that mass-dependent fractionation can, in principle, affect the accuracy of the mass-independent μ^{48}Ca data via inappropriate correction for the natural mass fractionation experienced by a sample. For example, correcting the natural mass-dependent fractionation using a kinetic law to retrieve the μ^{48}Ca data will result in the introduction of apparent effects (excess or deficit) in μ^{48}Ca if the natural fractionation is driven by non-kinetic processes34. Deviation from kinetic mass dependent fractionation can occur during calcite precipitation41 and during chemical weathering in arid environments42. The latter is relevant as a number of our samples are hot desert finds. Potential effects are on the order of up to 12 ppm on the μ^{48}Ca for a 0.1‰ effect on the $\delta^{42/44}$Ca value. The $\delta^{42/44}$Ca values we report here are in excellent agreement with literature data for the same group of meteorites (Extended Data Figure 3)43–45, confirming that potential effects from inadequate correction for natural mass-dependent fractionation are well within the uncertainty of our μ^{48}Ca measurements. Our $\delta^{42/44}$Ca data for individual chondrules from ordinary and CR chondrites are also comparable to that reported by for CV chondrites by Amsellem *et al.*44. Moreover, we find no systematics difference in the μ^{48}Ca values of hot desert and non-hot desert meteorite as well as falls versus finds in our dataset. In detail, μ^{48}Ca values for hot desert and non-hot desert meteorites as well as observed falls and finds from the same differentiated group (i.e. ureilites, angrites and Mars) are indistinguishable within uncertainty (Extended Data Figure 4). Additionally, potential effects on our data from addition of terrestrial Ca for lunar and martian meteorites can also be ruled out based on mass balance arguments. For example, accepting that the pristine martian μ^{48}Ca composition is -20±2.8 ppm relative to Earth, addition of 15% of terrestrial Ca, which would clearly be identifiable from hand specimens, would only result in a 3 ppm effect. This effect is well within the external reproducibility of our measurements. Given that the μ^{48}Ca composition of the Moon is even closer to Earth, addition of 15% terrestrial Ca to a lunar meteorite would results in even smaller effects relative to martian meteorites. Collectively, these data emphasize that the stable or mass-independent Ca isotope data are not affected by terrestrial processes prior to meteorite recovery within the uncertainty of our measurements.

Other nucleosynthetic isotope data in view of this model

Nucleosynthetic anomalies have been reported for number of elements aside from Ca (i.e. Ti, Cr, Ni, Sr, Nd, Mo, Ru and O)1,2,6,46–59 and, as such, we evaluate if our model is consistent with the isotope variability recorded in various Solar System reservoirs for these elements. In this exercise, we simply consider whether it is possible to generate the nucleosynthetic variability amongst inner Solar System bodies by admixing a CI-like composition to a depleted inner Solar System dust composition represented by ureilite

Europe PMC Funders Author Manuscripts

(where available) or angrite meteorites (Extended Data Figure 5). Based on published data1,2,6,46–54, we note that our model is compatible with the isotope variability observed for elements with a lithophile behavior such as ^{50}Ti, ^{54}Cr, ^{62}Ni, and ^{145}Nd within the uncertainties of the published data (Extended Data Figure 5). Nucleosynthetic anomalous isotopes of other elements either do not show significant variability beyond typical analytical uncertainties (i.e. ^{84}Sr)55–57, do not track the entire accretion history of planetary bodies (siderophile elements such as Mo, Ru)4 or are potentially affected by other processes such as gas-water interaction (oxygen). Thus, we conclude that our model is consistent with the nucleosynthetic variability that exists for elements that track the source of the silicate fraction of asteroidal and planetary bodies.

Europe PMC Funders Author Manuscripts

Extended Data

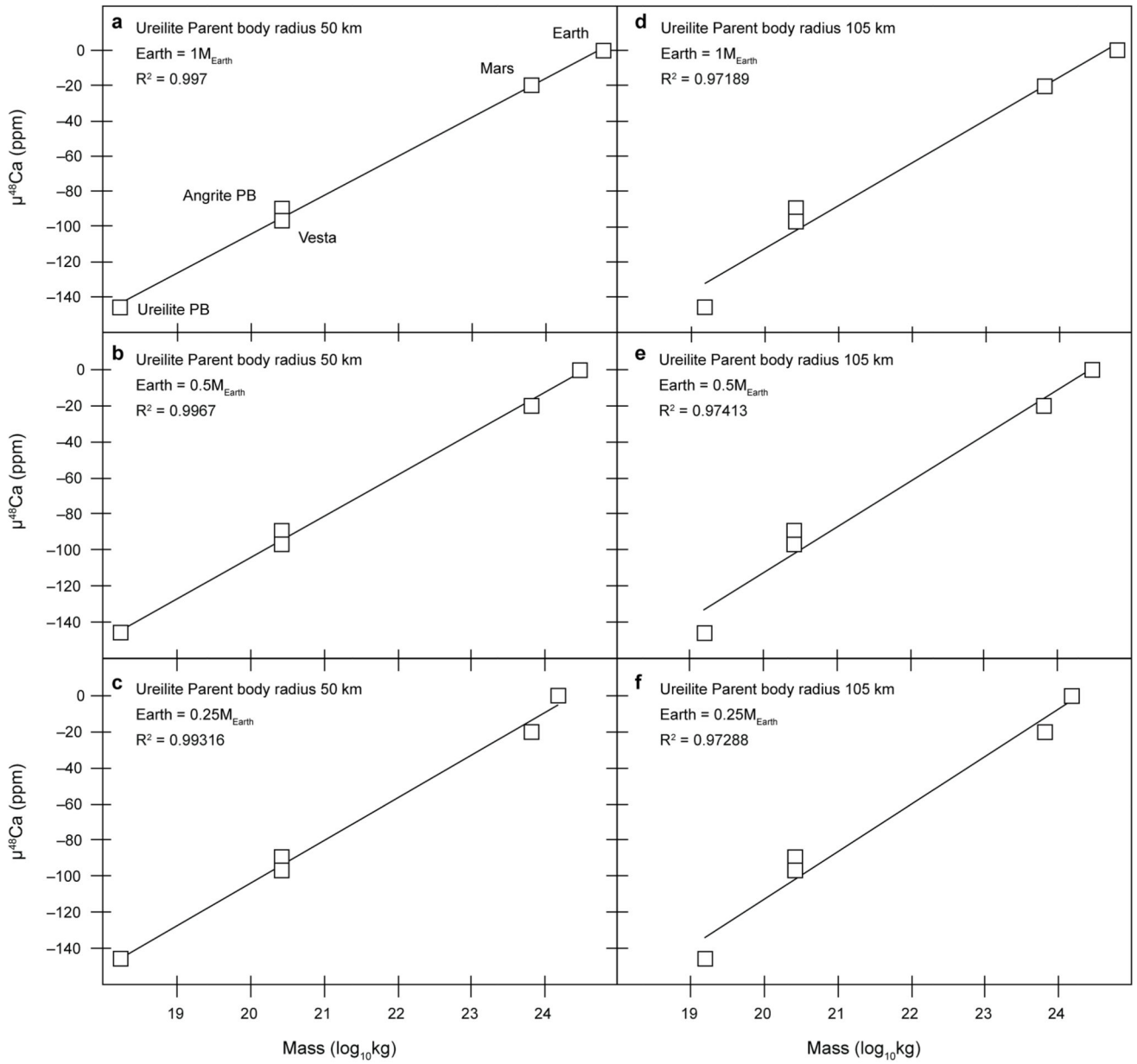

Extended Data Figure 1. The μ^{48}Ca composition of planetary bodies versus their mass with variable ureilite parent body and Earth's precursor masses.

Plots a-c show regressions and their correlation coefficients assuming an ureilite parent body with a radius of 50 km and masses for Earths' precursors of 1×M_{Earth}, 0.5×M_{Earth} and 0.25×M_{Earth}, respectively. Plots d-f show regressions assuming an ureilite parent body with a radius of 105 km and masses for Earths' precursors of 1×M_{Earth}, 0.5×M_{Earth} and 0.25×M_{Earth}, respectively. Masses for the angrite parent body, Vesta and Mars are the same as in figure 2A.

Europe PMC Funders Author Manuscripts

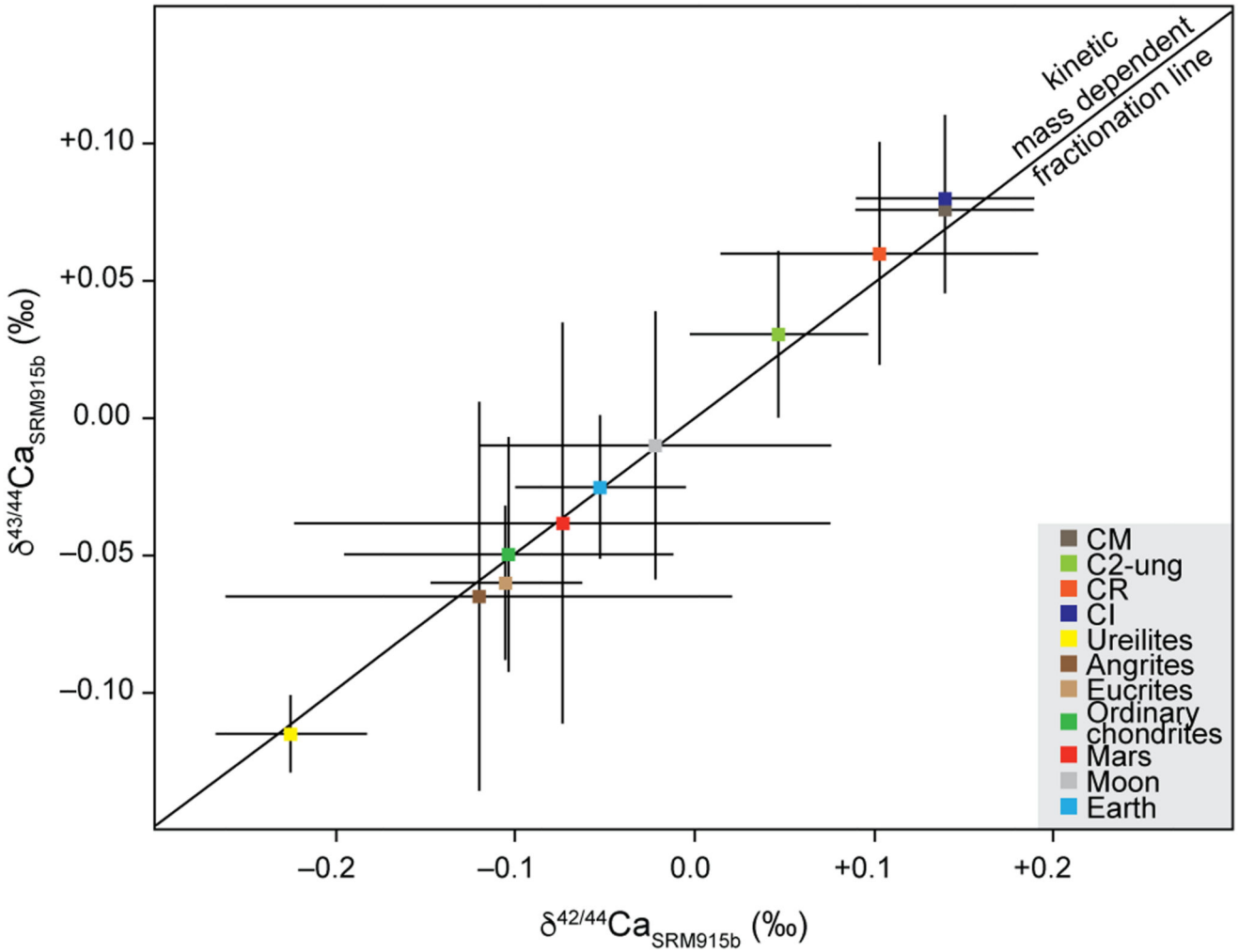

Extended Data Figure 2. Three isotope plot of reported average $\delta^{42/44}$Ca versus $\delta^{43/44}$Ca for Earth, meteorite parent bodies or chondrite groups relative to SRM 915b.

Shown also is the mass dependent fractionation line predicted by kinetic mass fractionation. Uncertainties are the 2SE of the mean of the analyzed samples per group. Where only a single sample represents the group, the error represents the external reproducibility (0.05 and 0.03 for $\delta^{42/44}$Ca versus $\delta^{43/44}$Ca, respectively) or the analytical uncertainty of the measurement, whichever is larger.

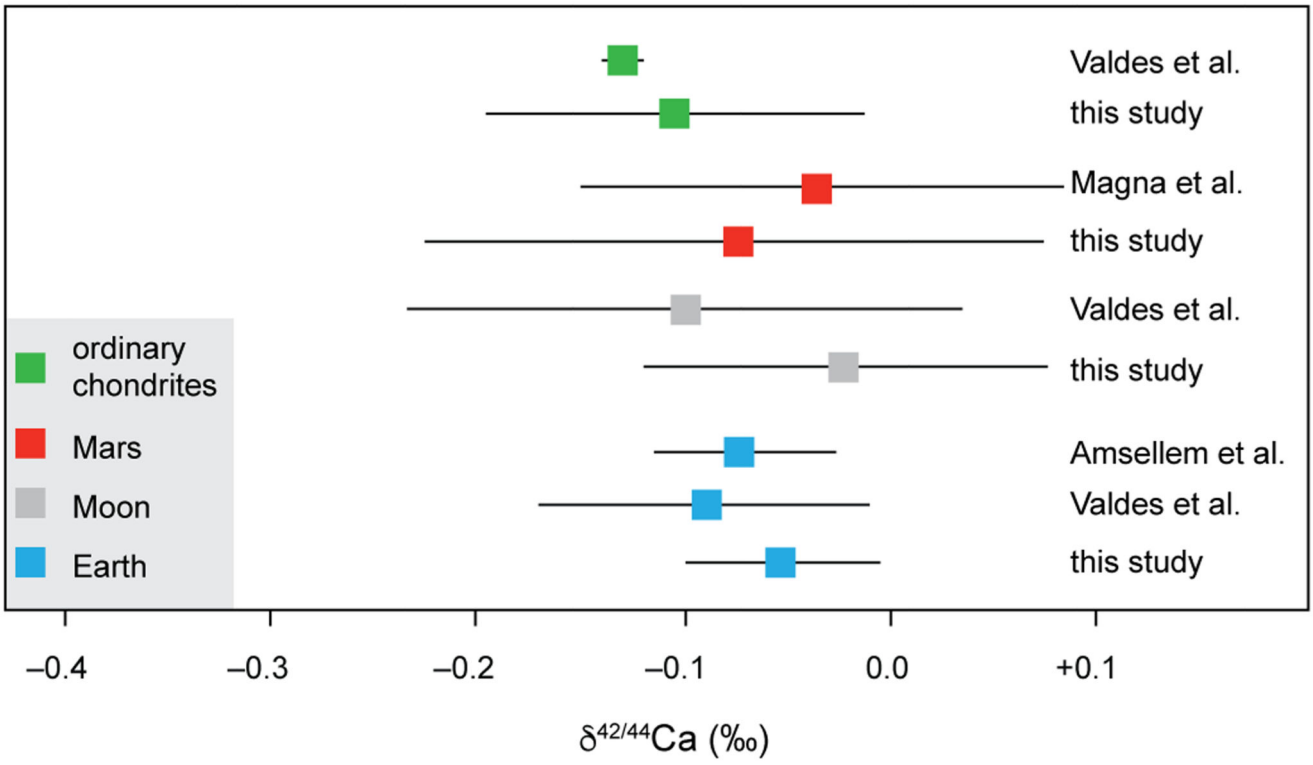

Extended Data Figure 3. Comparison of the $\delta^{42/44}$Ca values reported in the literature for ordinary chondrites, martian basalts, lunar and terrestrial basalts43–45 with those determined for the same types of samples in this study.

Europe PMC Funders Author Manuscripts

Europe PMC Funders Author Manuscripts

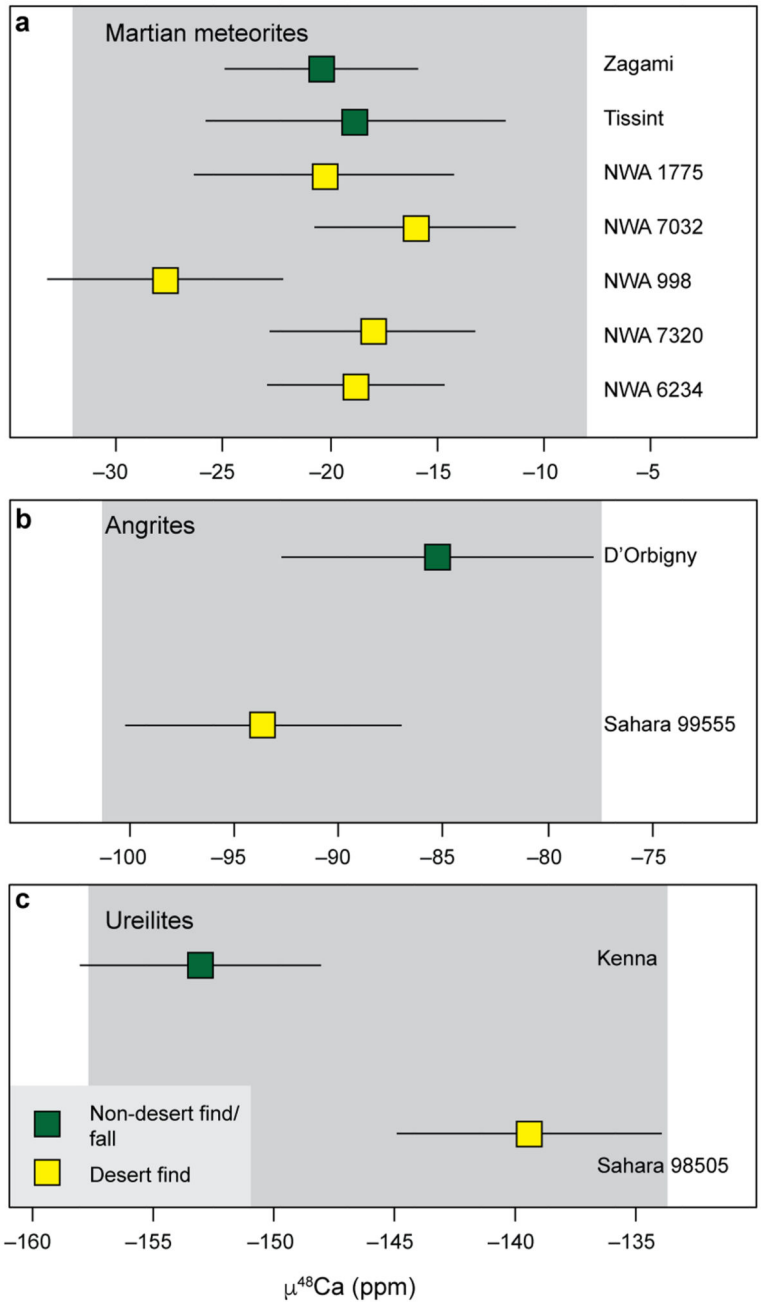

Extended Data Figure 4. Comparison of the μ^{48}Ca values determined for desert finds versus non-desert finds or falls.

Individual panels show data for (A) martian meteorites, (B) angrite meteorites and (C) ureilite meteorites. Grey bars indicate the external reproducibility of individual sample analyses.

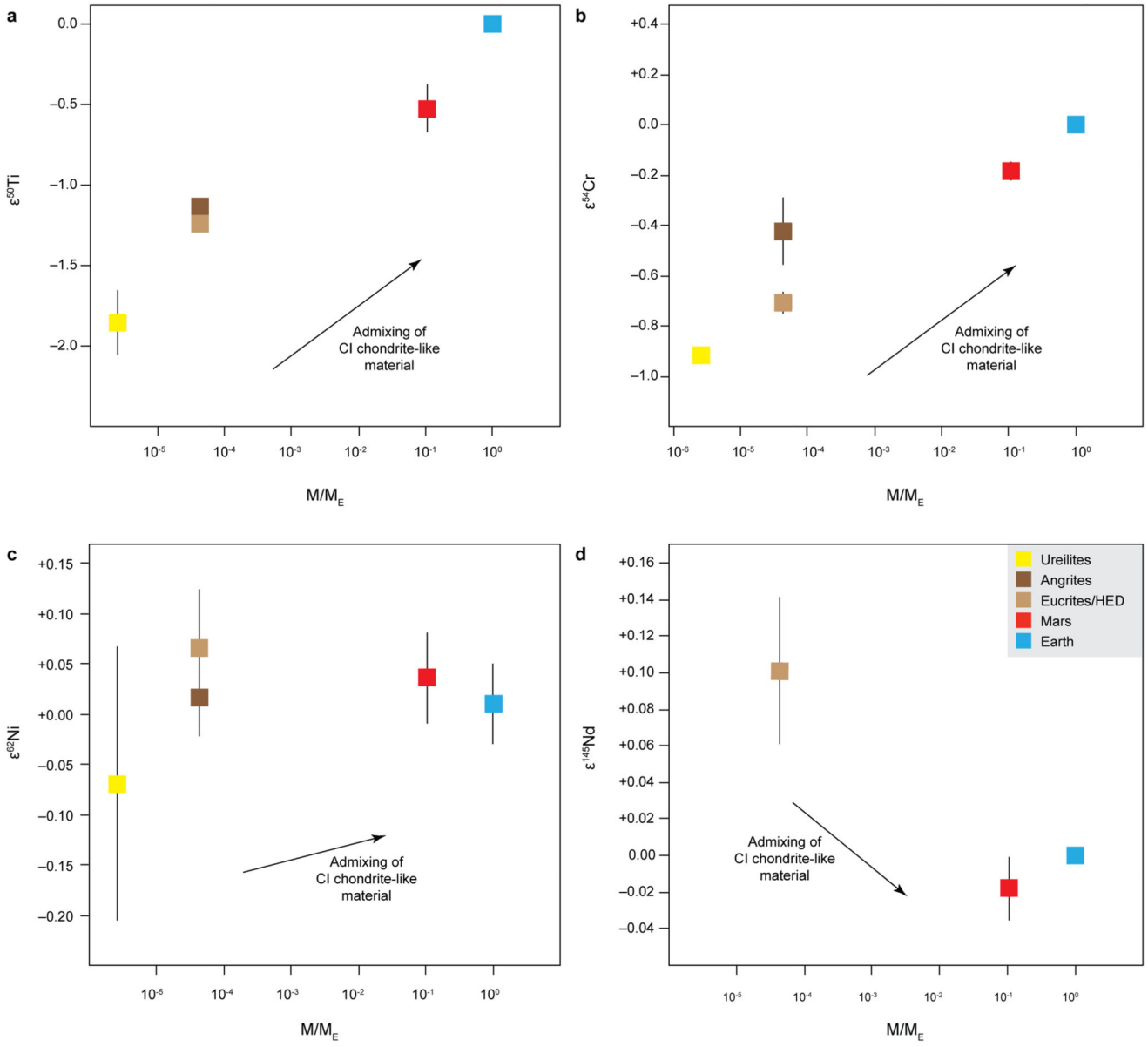

Extended Data Figure 5. Correlation of parent body mass, shown as mass relative to the mass of Earth (M/M_E), with nucleosynthetic anomalies for ^{50}Ti, ^{54}Cr, ^{62}Ni and ^{145}Nd reported in the literature1,2,6,46–54.

Indicated via arrows are the predicted effects of admixing of CI-like matter to the inner disk reservoir on the isotope composition based on measured nucleosynthetic signatures of CI chondrites.

Europe PMC Funders Author Manuscripts

Extended Data Table 1

Mass-independent $\mu^{48}Ca$ and mass dependent $\delta^{42/44}Ca$ and $\delta^{43/44}Ca$ data reported relative to SRM 915b.

Data marked with * are from ref. 3 and with † from ref. 34.

Sample	$\mu^{48}Ca \pm 2SE$	$\delta^{42/44}Ca \pm 2SE$	$\delta^{43/44}Ca \pm 2SE$
Earth			
BIR-1a (n=6)	+0.2 ± 1.7	−0.04 ± 0.02	−0.02 ± 0.01
BIR-1a†	+6.1 ± 5.7	−0.04 ± 0.02	−0.01 ± 0.02
BHVO-2†	+6.3 ± 7.5	−0.04 ± 0.04	−0.02 ± 0.02
BCR-2†	+5.2 ± 3.4	−0.08 ± 0.04	−0.04 ± 0.02
DNC-1†	+1.0 ± 4.0	−0.04 ± 0.03	−0.02 ± 0.01
BHVO-1†	−6.1 ± 8.1	−0.08 ± 0.03	−0.04 ± 0.02
SGR-1†	−4.6 ± 8.7	−0.02 ± 0.02	−0.01 ± 0.01
Sarm 40†	−6.7 ± 9.7	−0.08 ± 0.02	−0.04 ± 0.01
Mean	*+0.2 ± 3.9*	*−0.05 ± 0.02*	*−0.03 ± 0.01*
Moon			
NWA4734 (n=7)	+3.4 ± 6.7	−0.08 ± 0.04	−0.04 ± 0.02
Dhofar 026 (n=2)	+6.4 ± 2.5	+0.03 ± 0.00	+0.02 ± 0.00
NWA8632 (n=2)	+3.2 ± 3.3	+0.00 ± 0.13	+0.00 ± 0.06
Dhofar 287	+1.9 ± 4.7	−0.04 ± 0.03	−0.02 ± 0.02
Mean	*+3.7 ± 1.9*	*−0.02 ± 0.05*	*−0.01 ± 0.02*
Mars			
NWA6234	−18.8 ± 4.2	−0.03 ± 0.01	−0.01 ± 0.00
NWA 7320	−18.0 ± 4.8	−0.03 ± 0.02	−0.02 ± 0.01
NWA 998	−27.7 ± 5.5	−0.01 ± 0.01	−0.01 ± 0.00
NWA 7032	−16.0 ± 4.7	−0.02 ± 0.01	−0.02 ± 0.01
NWA 1775	−20.3 ± 6.1	−0.08 ± 0.04	−0.04 ± 0.02
Tissint	−18.8 ± 7.0	−0.22 ± 0.04	−0.11 ± 0.02
Zagami	−20.4 ± 4.5	−0.12 ± 0.04	−0.06 ± 0.02
Mean	*−20.0 ± 2.8*	*−0.07 ± 0.06*	*−0.04 ± 0.03*
Ordinary chondrites			
Kramer Creek (L4) (n=4)	−34.5 ± 10.7	−0.14 ± 0.07	−0.07 ± 0.03
Bovedy (L3)*	−35.4 ± 2.9	−0.13 ± 0.01	−0.06 ± 0.01
NWA 4910 (LL3)	−44.3 ± 9.3	−0.04 ± 0.01	−0.02 ± 0.01
NWA 5697 (L3) (n=3)	−25.5 ± 8.2	−0.11 ± 0.03	−0.05 ± 0.01
Mean	*−34.9 ± 7.7*	*−0.10 ± 0.05*	*−0.05 ± 0.02*
Eucrites			
Juvinas*	−91.5 ± 7.1	−0.12 ± 0.03	−0.07 ± 0.02
Stannern*	−102.4± 4.3	−0.09 ± 0.02	−0.05 ± 0.01
Mean	*−97.0 ± 10.9*	*−0.11 ± 0.03*	*−0.06 ± 0.02*
Angrites			
D'Orbigny*	−85.3 ± 7.5	−0.07 ± 0.02	−0.04 ± 0.01

Sample	μ^{48}Ca ± 2SE	$\delta^{42/44}$Ca ± 2SE	$\delta^{43/44}$Ca ± 2SE
Sahara 99555*	−93.6 ± 6.6	−0.17 ± 0.08	−0.09 ± 0.04
Mean	*−89.5 ± 8.3*	*−0.12 ± 0.10*	*−0.07 ± 0.05*
Ureilites			
Kenna*	−153.0 ± 5.0	−0.21 ± 0.01	−0.11 ± 0.01
Sahara 98505*	−139.4 ± 5.5	−0.24 ± 0.03	−0.12 ± 0.02
Mean	*−146.2 ± 13.6*	*−0.23 ± 0.03*	*−0.12 ± 0.01*
Carbonaceous chondrites			
Ivuna (CI)*	+206.1 ± 8.5	+0.14 ± 0.04	+0.08 ± 0.02
EET 92161 (CR2)	+222.5 ± 4.0	+0.07 ± 0.02	+0.05 ± 0.01
NWA 1180 (CR2)	+206.6 ± 4.6	+0.13 ± 0.01	+0.07 ± 0.00
Tagish Lake (C2-ung)	+291.3 ± 5.3	+0.05 ± 0.01	+0.03 ± 0.01
Jbilet Winselwan (CM2)	+314 ± 14	+0.14 ± 0.01	+0.08 ± 0.00
Chondrules			
NWA 5697 (LL3)			
2-C1	−150 ± 59	−0.20 ± 0.01	−0.08 ± 0.02
5-C2	−145 ± 53	−0.31 ± 0.10	−0.11 ± 0.04
5-C10	−51 ± 70	−0.19 ± 0.04	−0.08 ± 0.02
D-C3	−154 ± 10	+0.02 ± 0.05	+0.01 ± 0.03
5-C4	−15 ± 31	−0.33 ± 0.04	−0.15 ± 0.02
3-C5	−151 ± 16	−0.12 ± 0.04	−0.01 ± 0.00
11-C1	+16 ± 33	−0.19 ± 0.03	−0.08 ± 0.02
11-C2	−119 ± 24	−0.13 ± 0.01	−0.05 ± 0.02
3-C2	−101 ± 19	−0.10 ± 0.01	−0.05 ± 0.01
NWA 6043 (CR2)			
1-C2	+227 ± 16	−0.10 ± 0.01	−0.04 ± 0.01
2-C4	+198 ± 24	−0.06 ± 0.01	−0.04 ± 0.01

Acknowledgments

Financial support for this project was provided by the Danish National Research Foundation (DNRF97) and the European Research Council (ERC Consolidator Grant Agreement 616027 — STARDUST2ASTEROIDS) to M.B. V.A.F. acknowledges financial support via a DFG-Eigenstelle FE 1523/3-1 and the Royal Society for purchase of Dhofar 287. We thank Åke Nordlund, Anders Johansen and Frédéric Moynier for discussion on various aspects of this paper as well as James Day and an anonymous referee for constructive comments that greatly improved the quality of our paper.

References

1. Zhang J, Dauphas N, Davis AM, Leya I, Fedkin A. The proto-Earth as a significant source of lunar material. Nat Geosci. 2012; 5:251–255.
2. Trinquier A, et al. Origin of nucleosynthetic isotope heterogeneity in the solar protoplanetary disk. Science. 2009; 324:374–376. [PubMed: 19372428]
3. Schiller M, Paton C, Bizzarro M. Evidence for nucleosynthetic enrichment of the protosolar molecular cloud core by multiple supernova events. Geochim Cosmochim Acta. 2015; 149:88–102. [PubMed: 25684790]

4. Dauphas N. The isotopic nature of the Earth's accreting material through time. Nature. 2017; 541:521–524. [PubMed: 28128239]
5. Young ED, et al. Oxygen isotopic evidence for vigorous mixing during the Moon-forming giant impact. Science. 2016; 351:493–496. [PubMed: 26823426]
6. Burkhardt C, et al. In search of the Earth-forming reservoir: Mineralogical, chemical, and isotopic characterizations of the ungrouped achondrite NWA 5363/NWA 5400 and selected chondrites. Meteorit Planet Sci. 2017; 52:807–826.
7. Bollard J, et al. Early formation of planetary building blocks inferred from Pb isotopic ages of chondrules. Sci Adv. 2017; 3:e1700407. [PubMed: 28808680]
8. Ciesla FJ. Radial transport in the solar nebula: Implications for moderately volatile element depletions in chondritic meteorites. Meteorit Planet Sci. 2008; 43:639–655.
9. Lambrechts M, Johansen A. Rapid growth of gas-giant cores by pebble accretion. Astron Astrophys. 2012; 544:A32.
10. Johansen A, Mac Low MM, Lacerda P, Bizzarro M. Growth of asteroids, planetary embryos, and Kuiper belt objects by chondrule accretion. Sci Adv. 2015; 1:e1500109. [PubMed: 26601169]
11. Dauphas N, et al. Calcium-48 isotopic anomalies in bulk chondrites and achondrites: Evidence for a uniform isotopic reservoir in the inner protoplanetary disk. Earth Planet Sci Lett. 2014; 407:96–108.
12. Currie T, Sicilia-Aguilar A. The transitional protoplanetary disk frequency as a function of age: Disk evolution in the Coronet Cluster, Taurus, and other 1-8 Myr old regions. Astrophs J. 2011; 732:24.
13. McSween HY, et al. Dawn; the Vesta–HED connection; and the geologic context for eucrites, diogenites, and howardites. Meteorit Planet Sci. 2013; 48:2090–2104.
14. Wang H, et al. Lifetime of the solar nebula constrained by meteorite paleomagnetism. Science. 2017; 355:623–627. [PubMed: 28183977]
15. Schiller M, Baker JA, Bizzarro M. ^{26}Al–^{26}Mg dating of asteroidal magmatism in the young Solar System. Geochim Cosmochim Acta. 2010; 74:4844–4864.
16. Keil K. Angrites, a small but diverse suite of ancient, silica-undersaturated volcanic-plutonic mafic meteorites, and the history of their parent asteroid. Chem Erde. 2012; 72:191–218.
17. Macke RJ, Britt DT, Consolmagno GJ. Density, porosity, and magnetic susceptibility of achondritic meteorites. Meteorit Planet Sci. 2011; 46:311–326.
18. Wilson L, Goodrich CA, Van Orman JA. Thermal evolution and physics of melt extraction on the ureilite parent body. Geochim Cosmochim Acta. 2008; 72:6154–6176.
19. Wilson L, Keil K. Volcanic activity on differentiated asteroids: A review and analysis. Chem Erde. 2012; 72:289–321.
20. Schiller M, et al. Rapid timescales for magma ocean crystallization on the howardite-eucrite-diogenite parent body. Astrophs J Lett. 2011; 740:L22.
21. Schiller M, Connelly JN, Glad AC, Mikouchi T, Bizzarro M. Early accretion of protoplanets inferred from a reduced inner solar system ^{26}Al inventory. Earth Planet Sci Lett. 2015; 420:45–54. [PubMed: 27429474]
22. Bollard J, Connelly JN, Bizzarro M. Pb- Pb dating of individual chondrules from the CBa chondrite Gujba: Assessment of the impact plume formation model. Meteorit Planet Sci. 2015; 50:1197–1216. [PubMed: 27429545]
23. Dauphas N, Pourmand A. Hf–W–Th evidence for rapid growth of Mars and its status as a planetary embryo. Nature. 2011; 473:489–492. [PubMed: 21614076]
24. Hartmann L, Herczeg G, Calvet N. Accretion onto pre-main-sequence stars. Annu Rev Astron Astrophys. 2016; 54:135–180.
25. Kruijer TS, Burkhardt C, Budde G, Kleine T. Age of Jupiter inferred from the distinct genetics and formation times of meteorites. Proc Natl Acad Sci USA. 2017 201704461.
26. Picogna G, Kley W. How do giant planetary cores shape the dust disk? HL Tauri system. Astron Astrophys. 2015; 584:A110.
27. Carrasco-González C, et al. The VLA view of the HL Tau disk: Disk mass, grain evolution, and early planet formation. Astrophs J Lett. 2016; 821:L16.

28. Hartmann WK, Davis DR. Satellite-sized planetesimals and lunar origin. Icarus. 1975; 24:504–515.
29. Canup RM. Lunar-forming impacts: processes and alternatives. Phil Trans R Soc A. 2014; 372 20130175.
30. Canup RM. Forming a Moon with an Earth-like composition via a giant impact. Science. 2012; 338:1052–1055. [PubMed: 23076098]
31. Ćuk M, Stewart ST. Making the Moon from a fast-spinning Earth: a giant impact followed by resonant despinning. Science. 2012; 338:1047–1052. [PubMed: 23076099]
32. Meier MMM, Reufer A, Wieler R. On the origin and composition of Theia: Constraints from new models of the Giant Impact. Icarus. 2014; 242:316–328.
33. Kleine T, et al. Hf–W chronology of the accretion and early evolution of asteroids and terrestrial planets. Geochim Cosmochim Acta. 2009; 73:5150–5188.
34. Schiller M, Paton C, Bizzarro M. Calcium isotope measurement by combined HR-MC-ICPMS and TIMS. J Anal At Spectrom. 2012; 27:38–49.
35. Larsen KK, et al. Evidence for magnesium isotope heterogeneity in the solar protoplanetary disk. Astrophs J Lett. 2011; 735:L37.
36. van Kooten EM, Schiller M, Bizzarro M. Magnesium and chromium isotope evidence for initial melting by radioactive decay of ^{26}Al and late stage impact-melting of the ureilite parent body. Geochim Cosmochim Acta. 2017; 208:1–23.
37. Baker JA, Schiller M, Bizzarro M. ^{26}Al–^{26}Mg deficit dating ultramafic meteorites and silicate planetesimal differentiation in the early Solar System? Geochim Cosmochim Acta. 2012; 77:415–431.
38. Connelly JN, et al. The absolute chronology and thermal processing of solids in the solar protoplanetary disk. Science. 2012; 338:651–655. [PubMed: 23118187]
39. Estrada PR, Cuzzi JN, Morgan DA. Global modeling of nebulae with particle growth, drift, and evaporation fronts. I. Methodology and typical results. Astrophys J. 2016; 818:200.
40. Sugiura N, Fujiya W. Correlated accretion ages and ε^{54}Cr of meteorite parent bodies and the evolution of the solar nebula. Meteorit Planet Sci. 2014; 49:772–787.
41. Gussone N, et al. Calcium isotope fractionation in calcite and aragonite. Geochim Cosmochim Acta. 2005; 69:4485–4494.
42. Ewing SA, et al. Non-biological fractionation of stable Ca isotopes in soils of the Atacama Desert, Chile. Geochim Cosmochim Acta. 2008; 72:1096–1110.
43. Valdes MC, Moreira M, Foriel J, Moynier F. The nature of Earth's building blocks as revealed by calcium isotopes. Earth Planet Sci Lett. 2014; 394:135–145.
44. Amsellem E, et al. Testing the chondrule-rich accretion model for planetary embryos using calcium isotopes. Earth Planet Sci Lett. 2017; 469:75–83.
45. Magna T, Gussone N, Mezger K. The calcium isotope systematics of Mars. Earth Planet Sci Lett. 2015; 430:86–94.
46. Tang H, Dauphas N. Abundance, distribution, and origin of ^{60}Fe in the solar protoplanetary disk. Earth Planet Sci Lett. 2012; 359:248–263.
47. Tang H, Dauphas N. ^{60}Fe–^{60}Ni chronology of core formation in Mars. Earth Planet Sci Lett. 2014; 390:264–274.
48. Zhang J, Dauphas N, Davis AM, Pourmand A. A new method for MC-ICPMS measurement of titanium isotopic composition: Identification of correlated isotope anomalies in meteorites. J Anal At Spectrom. 2011; 26:2197–2205.
49. Trinquier A, Birck JL, Allegre CJ. Widespread ^{54}Cr heterogeneity in the inner solar system. Astrophys J. 2007; 655:1179.
50. Yamakawa A, Yamashita K, Makishima A, Nakamura E. Chromium isotope systematics of achondrites: Chronology and isotopic heterogeneity of the inner solar system bodies. Astrophys J. 2010; 720:150.
51. Qin L, Alexander CMD, Carlson RW, Horan MF, Yokoyama T. Contributors to chromium isotope variation of meteorites. Geochim Cosmochim Acta. 2010; 74:1122–1145.

52. Carlson RW, Boyet M, Horan M. Chondrite barium, neodymium, and samarium isotopic heterogeneity and early earth differentiation. Science. 2007; 316:1175–1178. [PubMed: 17525335]
53. Boyet M, Carlson RW. ^{142}Nd evidence for early (> 4.53 Ga) global differentiation of the silicate Earth. Science. 2005; 309:576–581. [PubMed: 15961629]
54. Borg LE, Brennecka GA, Symes SJ. Accretion timescale and impact history of Mars deduced from the isotopic systematics of martian meteorites. Geochim Cosmochim Acta. 2016; 175:150–167.
55. Moynier F, et al. Planetary-scale strontium isotopic heterogeneity and the age of volatile depletion of early Solar System materials. Astrophys J. 2012; 758:45.
56. Paton C, Schiller M, Bizzarro M. Identification of an ^{84}Sr-depleted carrier in primitive meteorites and implications for thermal processing in the solar protoplanetary disk. Astrophys J Lett. 2013; 763:L40.
57. Hans U, Kleine T, Bourdon B. Rb–Sr chronology of volatile depletion in differentiated protoplanets: BABI, ADOR and ALL revisited. Earth Planet Sci Lett. 2013; 374:204–214.
58. Clayton NR. Oxygen isotopes in meteorites. Annu Rev Earth Planet Sci. 1993; 21:115–149.
59. Fischer-Gödde M, Burkhardt C, Kruijer TS, Kleine T. Ru isotope heterogeneity in the solar protoplanetary disk. Geochim Cosmochim Acta. 2015; 168:151–171.

Europe PMC Funders Author Manuscripts

Europe PMC Funders Author Manuscripts

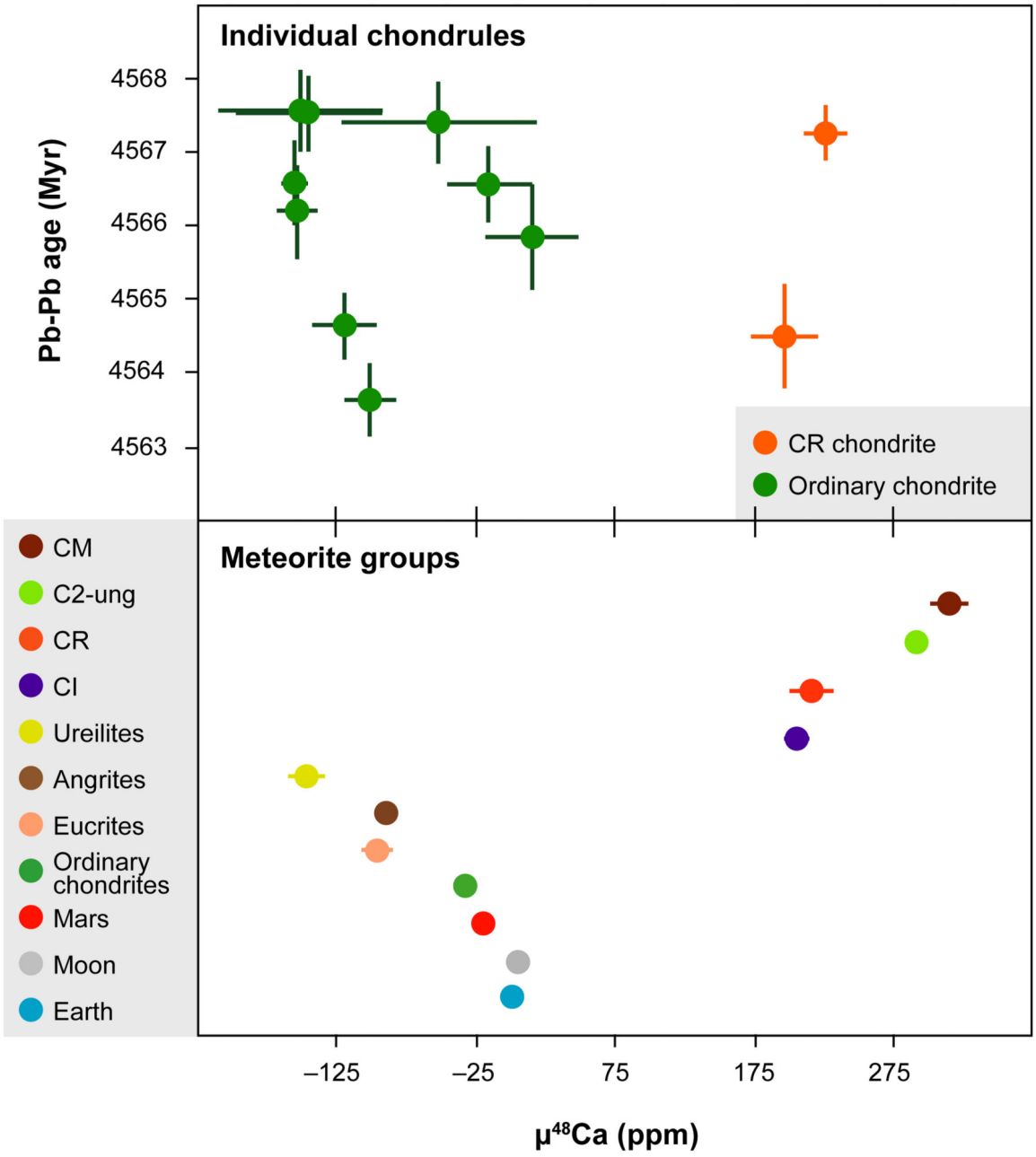

Fig. 1. Mass-independent ^{48}Ca data for individual chondrules and bulk meteorites.

Chondrule data are shown versus their Pb-Pb age7. Data are reported in the μ-notation where $\mu^{48}Ca = [(^{48}Ca/^{44}Ca)_{sample}/(^{48}Ca/^{44}Ca)_{SRM915b} - 1] \times 10^6$. Uncertainties are 2SE.

Europe PMC Funders Author Manuscripts

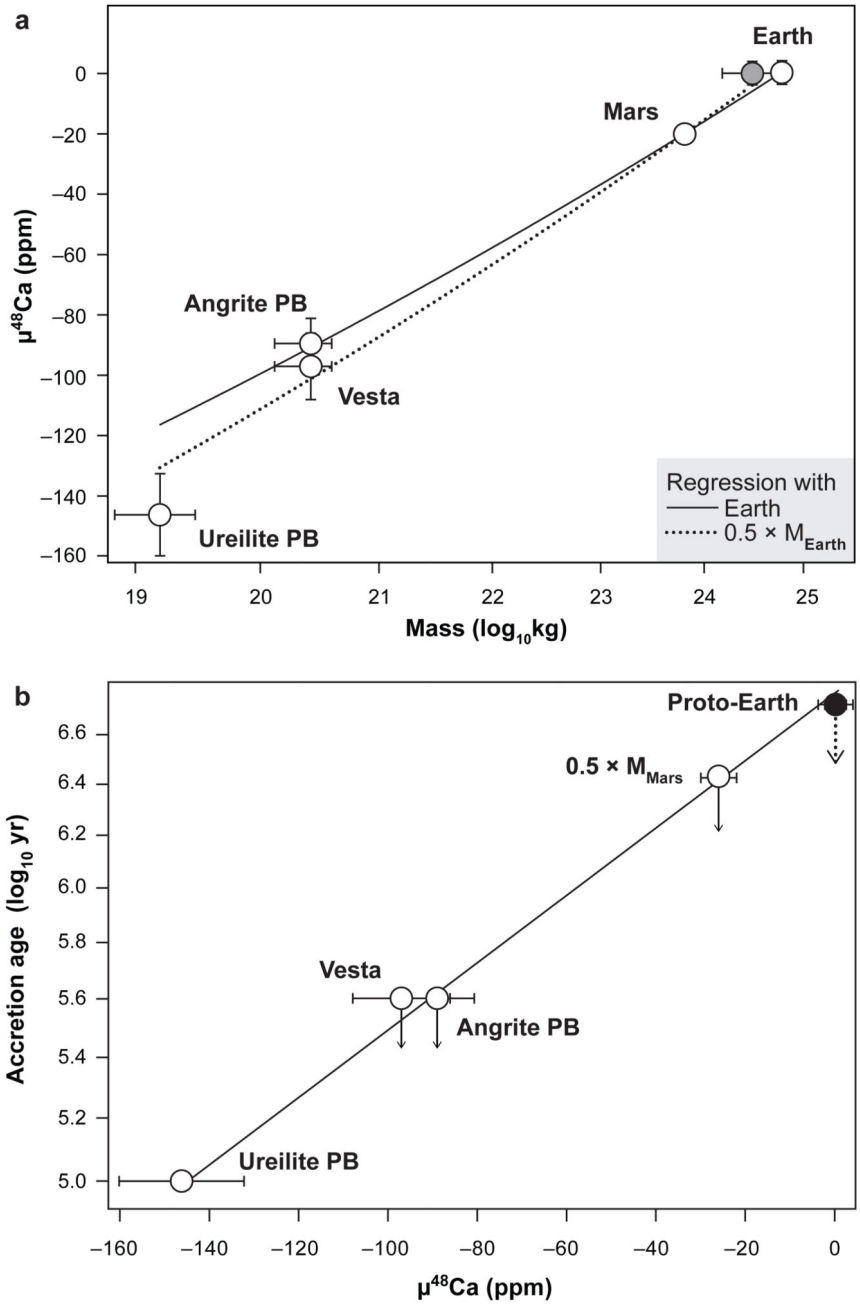

Fig. 2. The μ^{48}Ca composition of planetary bodies versus their mass and their maximum accretion age.

(A) Correlation of μ^{48}Ca composition of the ureilite parent body, Vesta, angrite parent body, Mars and the Earth with their respective masses on a logarithmic scale. The regression is a linear least-square fit ($y = a + b \times x$), where $a = -517.08 \pm 0.11$ and $b = 20.878 \pm 0.005$ (1SD). We assigned 50% uncertainty to the angrite parent body and the eucrite parent body (namely Vesta) masses. We also show a regression assuming a $0.50 \pm 0.25 \times M_{Earth}$ precursor (dash-dotted line). Regressions using alternative masses for the ureilite parent body and Earth (precursors) are shown in the Extended Data Figure 1. (B) Plot of the maximum accretion

ages of ureilite parent body, Vesta, angrite parent body and Mars at half of its current mass (see methods and ref. 20,21,23), shown in $\log_{10}$ yr after Solar System formation, versus the parent body μ^{48}Ca composition. Downward arrows indicate that accretion ages are upper limits. The linear regression with $a = 6.7232$ and $b = 0.011886$ is used to calculate the accretion age of proto-Earth at 5.3 Myr based on its μ^{48}Ca value. The accretion age of the proto-Earth likely reflects the accretion age of its precursors, which may include a number of planetary embyos. Thus, Earth's final accretion occurred after disk dissipation from colliding embryos. Note, however, that formation of a 0.9 Earth-mass object at 1 A.U. within 5 Myr is possible via pebble accretion10 although early accretion of proto-Earth is inconsistent the present-day W isotope composition of Earth's mantle33. However, a better understanding of the W isotope evolution of the proto-Earth in the framework of pebble accretion and a thourough assessment the extent of metal-silicate fractionation during the Moon-forming impact is required to assess this model. PB, parent body.

Europe PMC Funders Author Manuscripts

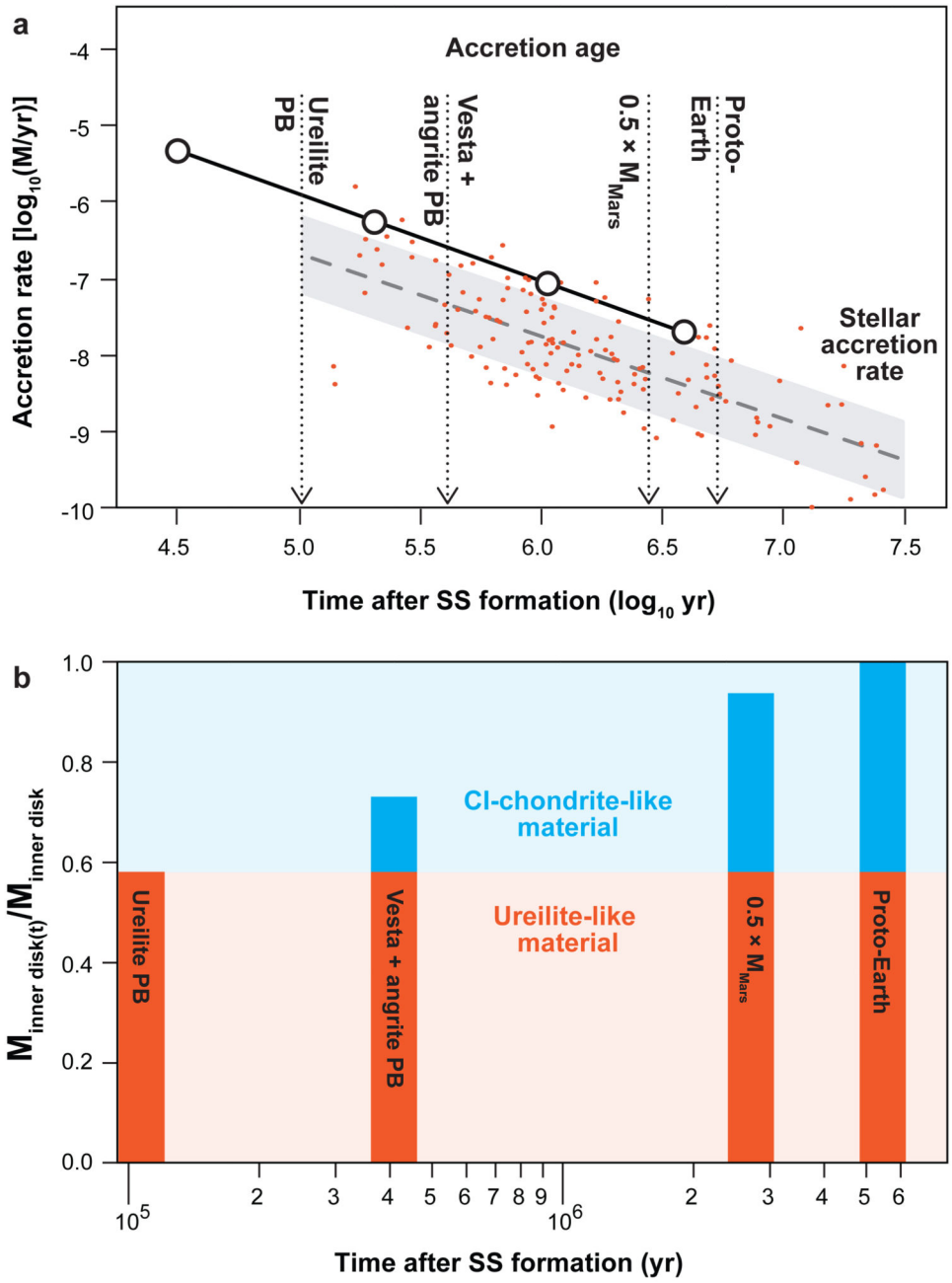

Fig. 3. Accretion rate of inner disk mass versus time.

Shown in (A) are the calculated accretion rates of the inner protoplanetary disk inferred from μ^{48}Ca composition and maximum accretion timescales of planetary bodies (white circles), assuming the μ^{48}Ca signature is representative of the entire inner disk mass at that time. Thus, the accretion rate of the inner protoplanetary disk reflects the amount of mass locked into bodies at any given time relative to the final disk mass, which is taken as the mass of asteroids, moons and planets located sunward of Jupiter (see methods). Given the apparent power law decline in our calculated accretion rates, we show the calculated values at

Δlog(*t*)/2 of their respective time interval. For comparison, we also show observed stellar accretion rates and the empirical accretion rate scaled to a 0.7 solar mass star versus time23. In (B), we show the proportion of mass locked into asteroids, embryos and planets at their maximum accretion age assuming that each parent body composition is representative of the bulk disk composition at the time of their accretion. The proportions are calculated as mixtures between a ureilite-like ^{48}Ca composition and outer Solar System dust represented by CI chondrites (see methods).

Europe PMC Funders Author Manuscripts